

1                   **Estimation of big sagebrush leaf area index with terrestrial laser scanning**

2

3   Peter J. Olsoy<sup>a,1</sup>, Jessica J. Mitchell<sup>b</sup>, Delphis F. Levia<sup>c</sup>, Patrick E. Clark<sup>d</sup>, and Nancy F. Glenn<sup>a,\*</sup>

4

5   <sup>a</sup>Boise State University, Department of Geosciences, Boise Center Aerospace Lab, 1910

6   University Drive, Boise, ID 83725, USA, peterolsoy@gmail.com, nancyglenn@boisestate.edu

7   <sup>b</sup>Appalachian State University, Department of Geography and Planning, P.O. Box 32066,

8   Boone, NC 28608, USA, mitchelljj@appstate.edu

9   <sup>c</sup>University of Delaware, Departments of Geography and Plant & Soil Sciences, 206 Pearson

10   Hall, Newark, DE 19716, USA, dlevia@udel.edu

11   <sup>d</sup>USDA Agricultural Research Service, 800 Park Blvd, Suite 105, Boise, ID 83712, USA,

12   pat.clark@ars.usda.gov

13

14   \* Corresponding author: Nancy F. Glenn, Boise State University, Department of Geosciences,

15   Boise Center Aerospace Lab, 1910 University Drive, Boise, ID 83725, USA,

16   nancyglenn@boisestate.edu, (208) 426-2933

17

18   <sup>1</sup> Present address: Washington State University, School of the Environment, 1228 Webster,

19   Pullman, WA 99164, USA

20 **Abstract**

21           Accurate monitoring and quantification of the structure and function of semiarid  
22 ecosystems is necessary to improve carbon and water flux models that help describe how these  
23 systems will respond in the future. The leaf area index (LAI,  $\text{m}^2 \text{m}^{-2}$ ) is an important indicator of  
24 energy, water, and carbon exchange between vegetation and the atmosphere. Remote sensing  
25 techniques are frequently used to estimate LAI, and can provide users with scalable  
26 measurements of vegetation structure and function. We tested terrestrial laser scanning (TLS)  
27 techniques to estimate LAI using structural variables such as height, canopy cover, and volume  
28 for 42 Wyoming big sagebrush (*Artemisia tridentata* subsp. *wyomingensis* Beetle & Young)  
29 shrubs across three study sites in the Snake River Plain, Idaho, USA. The TLS-derived variables  
30 were regressed against sagebrush LAI estimates calculated using specific leaf area  
31 measurements, and compared with point-intercept sampling, a field method of estimating LAI.  
32 Canopy cover estimated with the TLS data proved to be a good predictor of LAI ( $r^2 = 0.73$ ).  
33 Similarly, a convex hull approach to estimate volume of the shrubs from the TLS data also  
34 strongly predicted LAI ( $r^2 = 0.76$ ), and compared favorably to point-intercept sampling ( $r^2 =$   
35  $0.78$ ), a field-based method used in rangelands. These results, coupled with the relative ease-of-  
36 use of TLS, suggest that TLS is a promising tool for measuring LAI at the shrub-level. Further  
37 work should examine the structural measures in other similar shrublands that are relevant for  
38 upscaling LAI to the plot-level (i.e., hectare) using data from TLS and/or airborne laser scanning  
39 and to regional levels using satellite-based remote sensing.

40

41 **Keywords:** *Artemisia tridentata*, convex hull volume, ground-based LiDAR, leaf area index,  
42 terrestrial laser scanning, voxel volume

## 43 1. Introduction

44 Dryland ecosystems, including grasslands, shrublands, and savannas, occupy roughly  
45 40% of the Earth's land surface (Meigs, 1953) and are particularly sensitive to climate and land  
46 use change (Backlund et al., 2008). Vegetation dynamics in dryland ecosystems such as the  
47 sagebrush-steppe in the Great Basin of the United States will likely be affected by climate  
48 change through elevated levels of CO<sub>2</sub>, changes in air temperature, and the timing and  
49 distribution of precipitation (Bates et al., 2006; Kwon et al., 2008). In turn, woody plants such as  
50 sagebrush exert a major influence on dryland ecosystem processes such as evapotranspiration  
51 and carbon and nutrient cycling (Breshears, 2006; Yang, J. et al., 2012). Water and carbon fluxes  
52 in sagebrush are strongly related to plant leaf area index (LAI), a biophysical measure of the  
53 layers of leafy vegetation and an indicator of photosynthetic activity and net primary production  
54 (Bonan, 1993; Bussotti and Pollastrini, 2015; Smith et al., 1990). Changes in water and carbon  
55 cycling of the sagebrush-steppe in response to climate change will ultimately have land  
56 management consequences related to forage production, habitat quality and other ecosystem  
57 services (Polley et al., 2013). Importantly, measurement or accurate estimation of LAI is  
58 necessary for modeling and understanding water and carbon cycling in the sagebrush-steppe.

59 Due to their vast areal extent across North America, sagebrush (*Artemisia tridentata*  
60 Beetle)-dominated rangelands potentially represent a substantial carbon sink (Hunt Jr. et al.,  
61 2003; Prater and DeLucia, 2006). Understanding the spatiotemporal variability in sagebrush LAI  
62 is important for accurately predicting carbon budgets, even at the global scale (e.g., with global  
63 circulation models [GCMs]), under current and climate-change scenarios. Even within  
64 subspecies (e.g., Wyoming big sagebrush, *Artemisia tridentata* subsp. *wyomingensis* Beetle &  
65 Young), sagebrush LAI likely varies among plants, stands, and even regions as well as among

66 seasons and years. Data sets of sagebrush LAI for extensive areas and differing seasons are  
67 scarce because shrub LAI data are difficult and expensive to acquire with conventional field  
68 techniques (e.g., point-intercept sampling, light-intercept sensors, or destructive leaf harvest) and  
69 linkages that would promote upscaling between field measures and remotely-sensed estimates  
70 have not been established for shrublands (Hufkens et al., 2008). Consequently, accurate  
71 modeling of the spatiotemporal variability of sagebrush LAI is inhibited by a paucity of data to  
72 develop and validate such models over space and time. Without a better understanding of this  
73 spatiotemporal variability in sagebrush leaf area, accurate predictions of climate-change effects  
74 on sagebrush itself, and on water and carbon flux responses in sagebrush-dominated rangelands  
75 are not possible.

76         Efficient and accurate assessment techniques are important for facilitating sagebrush LAI  
77 data collection over extensive areas and among differing time periods. Many methods have been  
78 developed to estimate LAI in a variety of ecosystems. The most accurate estimates come from  
79 direct measurements that require destructive sampling (Beerling and Fry, 1990). Despite the  
80 advantages in increased accuracy with destructive sampling, it is time-intensive and impractical  
81 at scales relevant to modeling the impacts of climate change. Other direct measurements involve  
82 developing allometric equations related to easily measured vegetation characteristics such as  
83 height or canopy cover, or field techniques such as point-intercept sampling (Bonham, 1989;  
84 Clark and Seyfried, 2001). Indirect measurements usually involve light interception techniques  
85 with hemispherical photography (Jonckheere et al., 2004), or commercially available instruments  
86 such as the Li-Cor® LAI-2000 Plant Canopy Analyzer (Mussche et al., 2001). However, indirect  
87 estimates have proven challenging in sagebrush-dominated ecosystems because light is

88 disproportionately blocked by woody plant material, which leads to overestimation of LAI  
89 (Finzel et al., 2012).

90           Satellite remote sensing studies have demonstrated direct relationships between LAI and  
91 vegetation indices (Danson et al., 2003; Qi et al., 2000) such as the normalized difference  
92 vegetation index (NDVI) and the modified soil-adjusted vegetation index (MSAVI, Qi et al.,  
93 1994). These spectral indices leverage biophysical knowledge of the “red-edge” where  
94 photosynthetic absorption in the red spectrum and high reflectivity in the near-infrared correlate  
95 to green, leafy biomass or LAI (Turner et al., 1999). However, the relationship between  
96 vegetation indices and LAI breaks down in species with a large woody component (Hunt Jr. et  
97 al., 2003) and in dryland ecosystems in general because they contain weak vegetation signals  
98 overpowered by high soil reflectance and complex scattering (Kremer and Running, 1993;  
99 Mundt et al., 2006; Okin et al., 2001; Qi et al., 1994).

100           Terrestrial laser scanning (TLS) provides some advantages over standard field techniques  
101 for measuring or estimating sagebrush LAI, such as offering a link between ground-based  
102 measurements and airborne remotely-sensed estimates (Hopkinson et al., 2013; Vierling et al.,  
103 2013) and reduced personnel time cost per unit area sampled. Consequently, TLS could provide  
104 an effective means of acquiring the sagebrush LAI data needed to scale to satellite-based remote  
105 sensing and thus properly develop and validate ecological and hydrological models required to  
106 accurately understand and predict the consequences of climate change. To investigate the use of  
107 TLS for estimating LAI of Wyoming big sagebrush, a dominant sagebrush subspecies in the  
108 Great Basin, we: (1) assess the accuracy of using TLS data to derive vegetation metrics for  
109 estimating sagebrush LAI by comparing TLS metrics to those derived from destructive  
110 harvesting and leaf area field measurements; and (2) contrast the accuracy of the TLS-derived

111 sagebrush LAI with the field tested method of point-intercept sampling across three study sites in  
112 the Snake River Plain, Idaho, USA.

113 **2. Methods**

114 *2.1. Study Area*

115 The study was conducted at three sites across the Snake River Plain in southern Idaho,  
116 USA that are characteristic of the Snake River Plain and Northern Basin and Range ecoregions  
117 of the Great Basin; Reynolds Creek Experimental Watershed (RCEW), Hollister, and Snaky  
118 Canyon Wash (SCW). These sagebrush-grassland sites are dominated by Wyoming big  
119 sagebrush, bluebunch wheatgrass (*Pseudoroegneria spicata* A. Löve), and Sandberg bluegrass  
120 (*Poa secunda* J. Presl). The RCEW study site is located in Owyhee County (43°10'32"N,  
121 116°43'2"W; elevation: 1367 m) and has average annual precipitation of 271 mm and mean  
122 annual air temperature of 8.8 °C. Soils at RCEW consist of well-drained gravelly and silt loams  
123 from the Willhill-Cottle-Longcreek and Arbidge-Owsel-Gariper soil series complexes. The  
124 Hollister study site (Twin Falls County, Idaho, USA; 42°18'58"N, 114°41'34"W; elevation:  
125 1448 m) has average annual precipitation of 256 mm and mean annual temperature of 8.8 °C.  
126 The soil at Hollister is well-drained and consists of Chuska very stony loam and Shabliss silt  
127 loam. The SCW study site (Clark County, Idaho, USA; 44°4'23"N, 112°38'14"W; elevation:  
128 1529 m) has average annual precipitation of 206 mm, and mean annual temperature of 6.5 °C.  
129 Soils at SCW are somewhat excessively drained, gravelly loams from a complex of the  
130 Whitecloud, Simeroi, and Paint soil series. Climate data were sourced from the Western  
131 Regional Climate Center operated by the Desert Research Institute (WRCC, 2009), and soil data  
132 from Web Soil Survey of the Natural Resources Conservation Service (Soil Survey Staff, 2013).

133

134 2.2. Field Sampling

135 Terrestrial laser scanning, LAI point-  
136 intercept measurements, and destructive biomass  
137 sampling of Wyoming big sagebrush (hereafter  
138 referred to as sagebrush) was conducted at  
139 RCEW, Hollister and SCW from September to  
140 October 2012. Terrestrial laser scanning and  
141 destructive biomass sampling methods are  
142 detailed in Olsoy et al. (2014). Scanning was  
143 performed with a Riegl VZ-1000 TLS instrument  
144 with a 1550 nm near-infrared laser with  
145 waveform processing, 8 mm accuracy at 100 m  
146 range (Riegl, 2015), and a beam diameter of 2  
147 mm at 6.67 m range (Yang, R. et al., 2012).  
148 Three plots were established at each study site  
149 and each plot contained two 25 m<sup>2</sup> sub-plots. The  
150 sub-plots all included two or three marked  
151 sagebrush ( $n = 15$  per site, total  $n = 45$ ) and were  
152 scanned from two opposing scan positions at a  
153 mean distance of 5.7 m from each sagebrush  
154 plant with laser pulse rate set to 300 kHz and an  
155 angular stepwidth of 0.01°, resulting in a minimum point spacing of 2 mm (**Fig. 1**). Scans were  
156 georeferenced using four reflective targets whose positions were captured using a survey-grade

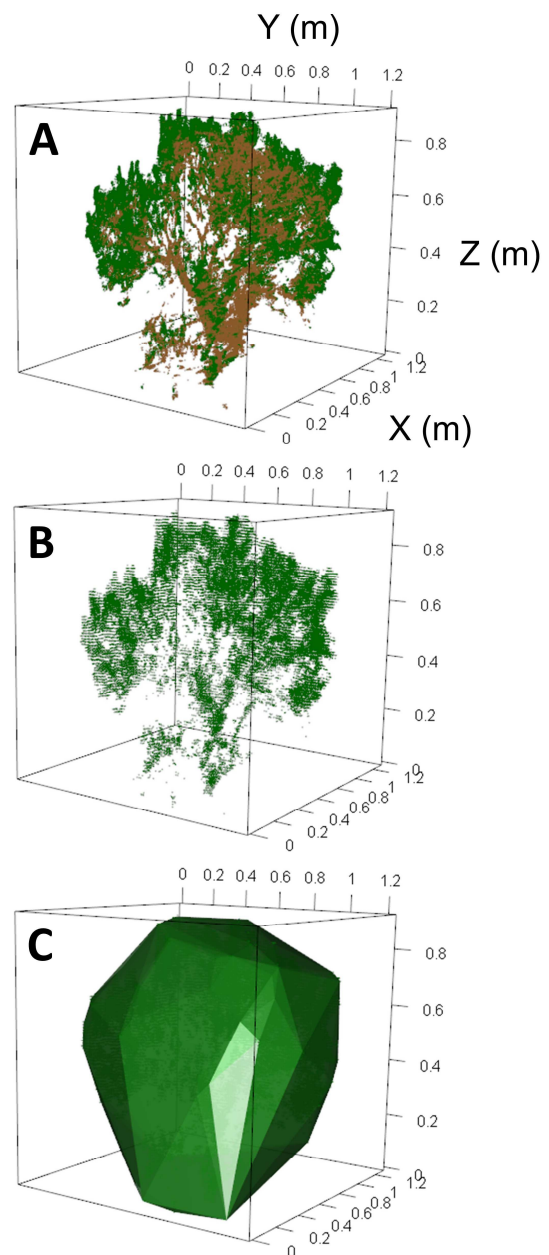


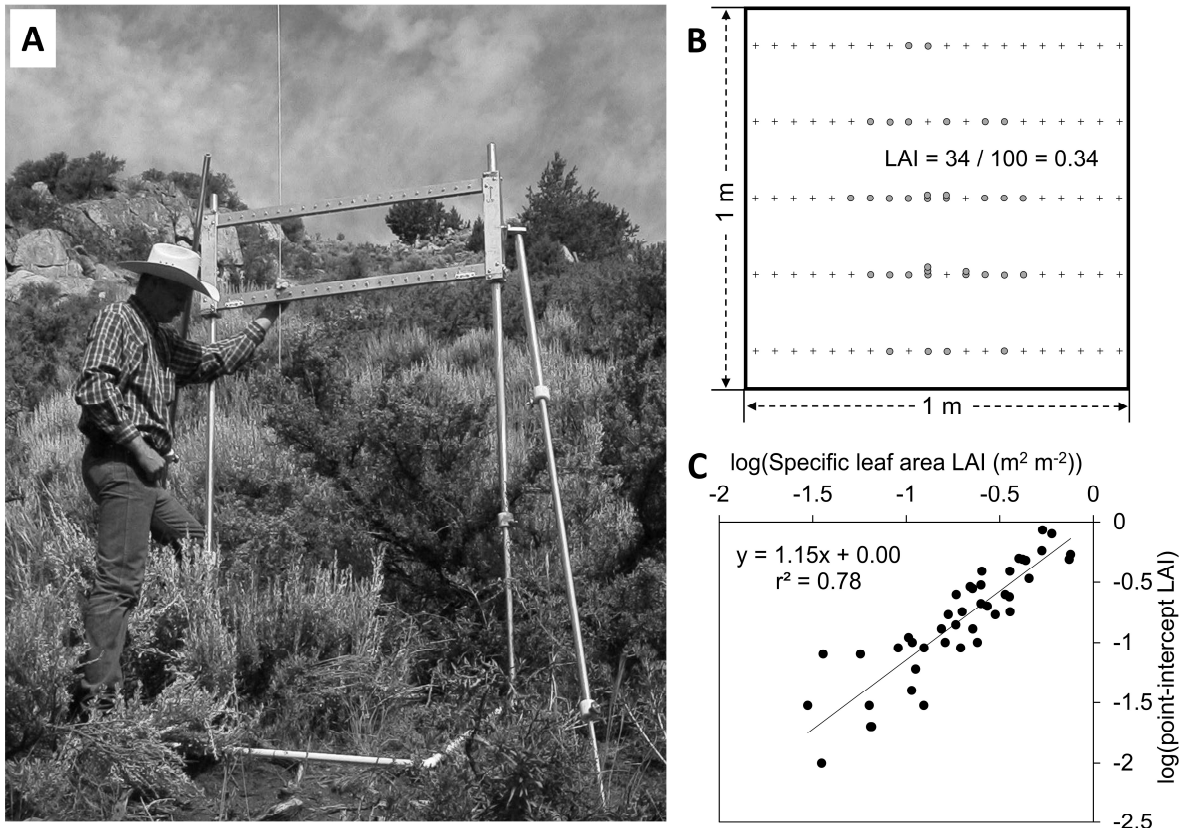
**Figure 1.** Point cloud of a sagebrush with green and non-green classified points (A); voxelized green volume (B); and convex hull green volume (C).



157 GPS unit. After scanning the sub-plots, a 1-m<sup>2</sup> quadrat ( $n = 42$ ) was fit around each sagebrush  
158 within the sub-plots and point-intercept sampling was applied to estimate LAI (Clark and  
159 Seyfried, 2001). The sagebrush LAI point-intercept sampling approach uses a 20-pin frame with  
160 five equally spaced frame locations within the 1 m<sup>2</sup> quadrat for a total of 100 attempts m<sup>-2</sup>. This  
161 method uses a sharpened pin that is pushed through the sagebrush canopy and one records the  
162 number of pin-point contacts or “hits” with green foliage. The number of green hits is divided by  
163 the number of attempts to give an estimate of LAI (**Fig. 2**). Multiple point frames may be used  
164 for shrubs larger than 1 m<sup>2</sup>. However, in this study, shrubs that did not fit within a single quadrat  
165 (i.e., > 1 m<sup>2</sup>) were excluded from the LAI analysis due to limitations of comparing multiple point  
166 frames with metrics from a single TLS point cloud.

167         After point-intercept sampling, each sagebrush was destructively sampled by cutting the  
168 sagebrush at ground-level and collecting the plant matter into plastic bags for temporary storage.  
169 All samples were sorted to separate the green biomass; which included leaves, green stems, and  
170 seeds, from the woody biomass. The sorted samples were oven-dried at 65 °C for 48 h or until a  
171 constant dry weight was reached and recorded. The biomass of the green and woody components  
172 were recorded separately for each sagebrush plant (Olsoy et al., 2014).

173         In January and February 2014, sagebrush leaves were collected at the three sites to obtain  
174 site-wide specific leaf area (cm<sup>2</sup> g<sup>-1</sup>, SLA) for estimation of LAI from field-measured biomass.  
175 The sagebrush leaf data collection consisted of collecting a total of 400 fresh leaves from each  
176 study site. For each study site, 100 leaves were collected at random from multiple shrubs (5–15  
177 shrubs) at each of the three plots and an additional 100 leaves were randomly collected from all  
178 of the combined plots. The combined sample for each study site was maintained separately and  
179 later used to independently validate mean SLA values.



180

181 **Figure 2.** Photo of point-intercept sampling being performed in the field (A). A schematic showing the number of

182 attempted pin-point hits (crosses) in a 1 m<sup>2</sup> quadrat with theoretical distribution of green hits (grey circles) (B).

183 Regression results for point-intercept LAI plotted against specific leaf area LAI (C).

184

### 185 2.3. Lab Analysis

186 Sagebrush specific leaf area was calculated for shrubs located at all nine of the plots

187 (RCEW, Hollister, and SCW) following standard procedures outlined by Breda (2003). Briefly, a

188 sub-sample of leaves collected from sagebrush plants at the study sites were used to calculate SLA,

189 which is a site-specific ratio of leaf area to dry leaf biomass (Chiarriello et al., 1989). Multiplying

190 the measured dry leaf biomass of a plant by the site-specific SLA provides an estimate of leaf area

191 for each sampled plant.

192 Collected leaves were stored at 0 °C until processed 1–2 days later. The total surface area  
193 (cm<sup>2</sup>) of all collected leaves for each individual or combination plot was determined with a Li-  
194 Cor 3100 Leaf Area Meter (1 mm<sup>2</sup> resolution) with an error of ±1% for a 10 cm<sup>2</sup> area. The leaf  
195 area meter was calibrated with the factory supplied calibration disk between runs. The leaf  
196 samples were bagged by plot, oven-dried in a laboratory-grade gravity convection oven for 48 h  
197 at 80 °C, and weighed to the nearest thousandth of a gram. The SLA of each plot was then  
198 calculated as the quotient of surface area and oven-dry weight. The site-specific SLA values  
199 were multiplied by the green biomass dry-weight of each sagebrush plant to obtain an estimated  
200 leaf area and divided by the sampled ground surface area to convert into a dimensionless  
201 parameter of LAI. The point-intercept LAI estimates and TLS-derived vegetation metrics were  
202 then compared to this SLA-derived LAI estimate.

203 Specific leaf area is often used as an indicator of photosynthetic efficiency or resource  
204 allocation by plants (Reekie and Reekie, 1991). Stressors such as low water availability and  
205 animal browsing can cause plants to compromise between photosynthesis and growth (Hoffman  
206 and Wambolt, 1996). We assumed that SLA would not differ between 2012, when field sampling  
207 was performed, and 2014, when SLA sampling was performed. This assumption is similar to  
208 another study which considered SLA to be consistent at a site across different years (e.g., Turner  
209 et al., 1999). SLA is largely governed by site-specific properties, such as soil fertility, solar  
210 insolation, and precipitation (Ackerly et al., 2002; Ordoñez et al., 2009), which may differ  
211 between years.

212

#### 213 2.4. TLS Analysis

214 The scans from the TLS were registered together in RiSCAN Pro software (Riegl Laser  
215 Measurement Systems GmbH, Horn, Austria). Each shrub was manually delineated to remove  
216 laser hits or points on the ground surface and on non-target vegetation. The point cloud was post-  
217 processed to remove noisy points that represent partial or false returns using a Riegl-specific  
218 metric referred to as “deviation”, which is a measure of the difference in pulse shape of the laser  
219 return compared to the emitted pulse (Greaves et al., 2015; Pfennigbauer, 2010). All points were  
220 used to calculate shrub height and canopy cover. We determined canopy cover by calculating the  
221 percent of the ground surface covered using a minimum convex polygon of the TLS points.  
222 Shrub height and canopy cover were multiplied together as an alternative to voxel and convex  
223 hull volume. The remaining points were classified using the methods described in Olsoy et al.  
224 (2014), where points with laser-reflectance values below a given threshold are classified as  
225 green, or photosynthetically active (see also Beland et al., (2014) for similar TLS reflectance-  
226 based classification of leaf points). The subset of green-classified points was then used to  
227 calculate canopy volume using a voxel-based approach and a 3-D convex hull approach (Olsoy  
228 et al., 2014). Voxels are volumetric pixels of a given size (e.g., 1 cm<sup>3</sup>) that are either counted (1)  
229 or not (0) based on whether they contain points (Greaves et al., 2015; Hosoi and Omasa, 2006;  
230 Olsoy et al., 2014). The convex hull approach uses the outermost set of points to create a volume  
231 (Barber et al., 1996; Olsoy et al., 2014). These two approaches alternatively provide a minimum  
232 (voxels, **Fig. 1B**) and maximum (convex hull, **Fig. 1C**) volume for each plant. Finally, the green-  
233 classified points were also multiplied by the average beam area to obtain a direct estimate of TLS  
234 leaf area (m<sup>2</sup>). The average beam area for each sagebrush was estimated based on the distance  
235 between the plant and the scanner and assuming a uniform beam divergence for each plant.

236 2.5. Statistical Analysis

237 To compare the accuracy of TLS-derived metrics to point-intercept sampling, each  
238 variable (height, canopy cover, volume, and TLS leaf area) was regressed against the SLA-  
239 derived LAI estimate (SLA LAI). In all cases, the residuals and variance were non-normal,  
240 therefore both the response and independent variables were log-log transformed giving (Eq. 1):

$$241 \log(L) = k\log(x) + a$$

242 where,  $L$  is SLA LAI,  $k$  and  $a$  are the regression slope and intercept parameters, and  $x$  is the  
243 independent variable. Back-transforming gives the power law equation (Eq. 2):

$$244 L = 10^a x^k$$

245 Power law equations are frequently found in biological systems with allometric scaling (Enquist  
246 et al., 1998). For example, sagebrush and global inflorescence biomass have been compared to  
247 stem and leaf biomass using log-log transformations of the data (Cleary et al., 2008). Another  
248 example is a common allometric function - the logarithmic relations between diameter at breast  
249 height or basal area and leaf area index, which produces a power law relation between mass per  
250 dry weight or area and stem diameter (Gower et al., 1999; Levia, 2008; Whittaker and  
251 Woodwell, 1967).

252 An analysis of variance (ANOVA) was used to test the site-specificity of our sagebrush  
253 SLA measurements at our three study sites across the Snake River Plain. All statistical tests were  
254 performed with the R statistical package (R Core Team, 2013). Test assumptions were evaluated  
255 with a Shapiro-Wilk normality test and a Bartlett test of homogeneity of variance. The one-way  
256 ANOVA test determined if the means at the sites were all equal, and a Tukey's honest significant  
257 difference test was then used to further analyze which pairs of means differed from each other.

### 258 3. Results and Discussion

#### 259 3.1. Specific Leaf Area

260 Specific leaf area values at Hollister ( $42.3 \pm 3.93 \text{ cm}^2\text{g}^{-1}$ ) and SCW ( $42.2 \pm 6.49 \text{ cm}^2\text{g}^{-1}$ )  
261 were larger than at RCEW ( $30.1 \pm 2.03 \text{ cm}^2\text{g}^{-1}$ ;  $P = 0.025$ ). Specific leaf area was thus found to  
262 be site-specific for sagebrush, similar to previous studies. For example, a study of sagebrush in  
263 Yellowstone National Park reported SLA of  $45.2 - 54.6 \text{ cm}^2\text{g}^{-1}$  (Hoffman and Wambolt, 1996).  
264 Another dryland shrub, *Retama sphaerocarpa* (Boiss.), had SLA ranging from about 14 to 16  
265  $\text{cm}^2\text{g}^{-1}$  (Pugnaire et al., 1996). The lower SLA values at RCEW indicate thicker leaves, which  
266 contributes to a longer leaf life span, improved nutrient retention and protection of the leaves  
267 from desiccation (Ackerly et al., 2002; Poorter and Remkes, 1990). These plant adaptations may  
268 dampen the turnover of evapotranspiration (ET), which has been reported to return as much as  
269 90% of incoming precipitation to the atmosphere (Branson et al., 1976; Flerchinger et al., 1996;  
270 Wight et al., 1986). Overall, the significant differences in SLA in this study are likely attributed  
271 to some combination of differences in genetic variation, phenological development and  
272 environmental factors (e.g., microhabitat features) across the study sites. Ongoing work at the  
273 Hollister and RCEW sites includes more intensive SLA sampling that is concurrent with airborne  
274 hyperspectral (AVIRIS-NG) image acquisitions to explore spectral estimates of SLA on a per  
275 pixel basis. Several recent studies have demonstrated the use of spectral data collected or  
276 simulated at the leaf scale to estimate SLA in boreal forests (Serbin et al., 2014), leaf mass per  
277 unit area (the inverse of SLA) across a range of species (Cheng et. al., 2014) and live fuel  
278 moisture content and leaf dry mass in sagebrush (Qi et al., 2014). While sagebrush SLA values  
279 also fluctuate seasonally, future studies could minimize the influence of forbs and grasses on  
280 shrub LAI estimation error by sampling in late summer and early fall after senescence.

281

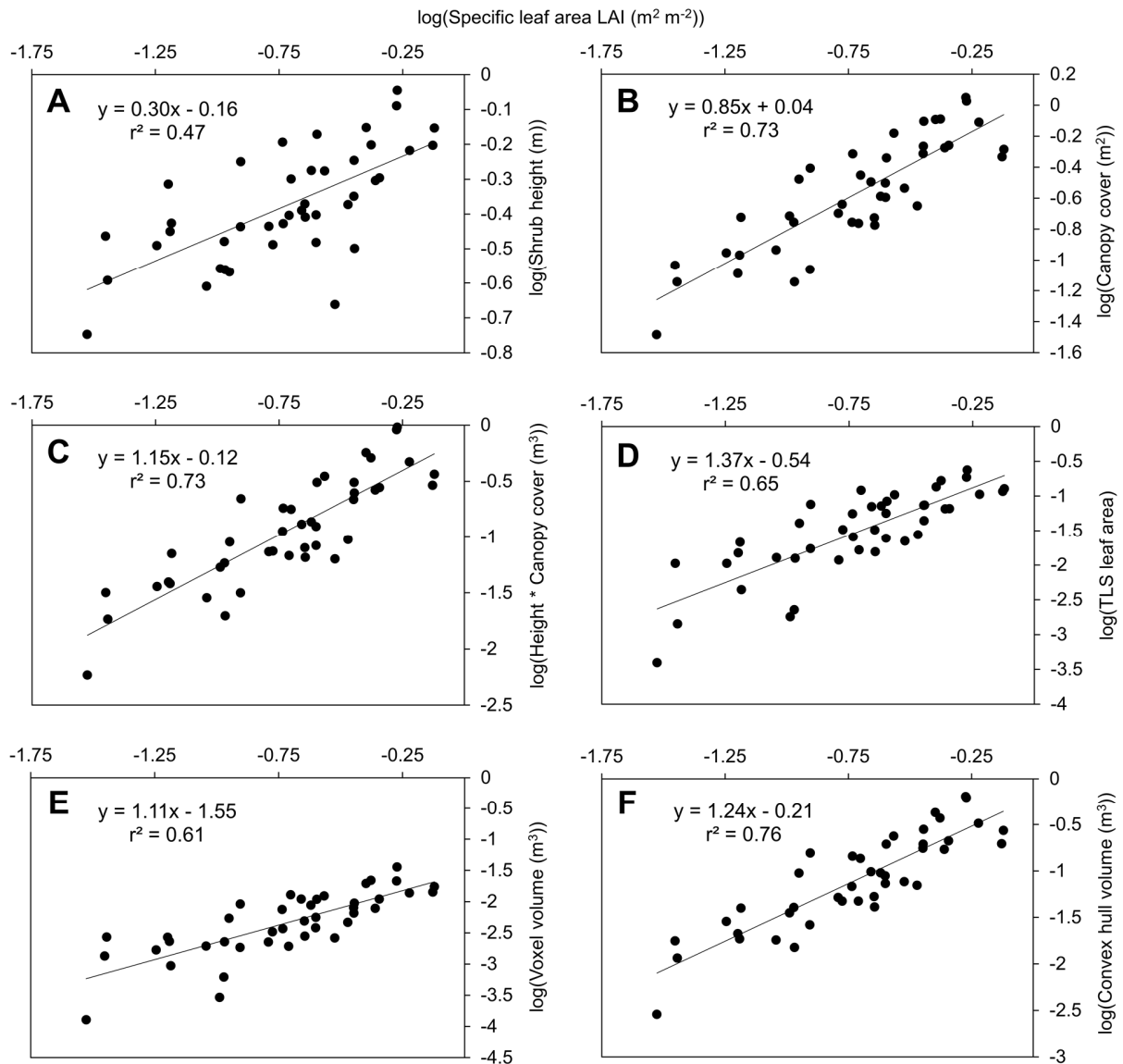
### 282 3.2. LAI Estimation

283 TLS-derived vegetation metrics and field-based point-intercept sampling performed  
284 similarly well when compared against SLA-derived LAI as a standard (**Figs. 2C and 3**). Canopy  
285 volumetric estimates derived from TLS performed well when regressed against SLA LAI, with  
286 3-D convex hull providing the highest estimates ( $r^2 = 0.76$ , **Fig. 3F**), while 1 cm<sup>3</sup> voxel volume  
287 explained 61% of the variation ( $r^2 = 0.61$ , **Fig. 3E**). Shrub height estimates were a relatively poor  
288 predictor of LAI ( $r^2 = 0.47$ , **Fig. 3A**) compared to canopy cover ( $r^2 = 0.73$ , **Fig. 3B**).  
289 Multiplying shrub height and canopy cover together provided no added benefit over canopy  
290 cover alone ( $r^2 = 0.73$ , **Fig. 3C**). A direct estimate of leaf area from the green-classified points  
291 explained 65% of the variation in SLA LAI ( $r^2 = 0.65$ , **Fig. 3D**). Finally, point-intercept  
292 sampling explained almost 80% of the variation ( $r^2 = 0.78$ , **Fig. 2C**). Clark and Seyfried (2001)  
293 found similar results in sagebrush communities using point-intercept sampling with vertical pins  
294 ( $r^2 = 0.82$ ). The direct estimate using green-classified points may have been less effective than  
295 expected due to incomplete penetration of the TLS into the shrub canopy. In addition, one  
296 potential reason that TLS-derived convex hull volume did not improve on point-intercept  
297 sampling is that the volumetric measurement provided by the convex hull does not account for  
298 within canopy variation. This could be problematic for larger shrubs, which were excluded from  
299 our analysis. Therefore, study sites with a dominance of larger shrubs (> 1 m<sup>2</sup>) require further  
300 validation and possibly the use of other volumetric methods.

301 Voxel size must be chosen with consideration of beam diameter, leaf size, and  
302 distribution of leaves (Beland et al., 2014; Cifuentes et al., 2014; García et al., 2015). Greaves et  
303 al. (2015) demonstrated that slightly larger voxels (3-5 cm,  $R^2 > 0.9$ ) from TLS greatly improved  
304 biomass estimation of two arctic shrub species (*Salix pulchra* Cham. and *Betula nana* L.) in

305 northern Alaska compared to 1 cm<sup>3</sup> voxels ( $R^2 = 0.38$ ). Further, Greaves et al. (2015) found that  
306 for variable-range point clouds, a volume differencing approach was more effective than voxel  
307 counting. However, Hosoi and Omasa (2007) used smaller 5 mm voxels with TLS to  
308 successfully model leaf area density throughout the canopy of a mixed tree plantation in Tokyo,  
309 Japan, with mean absolute error of 12.7% when measurement zenith angle was 90° compared to  
310 57% error at 71°, suggesting that incidence angle may be just as important as voxel size. Beland  
311 et al. (2014) recommended voxels approximately 10 times the leaf size to minimize occlusion  
312 while retaining the detailed structural information inherent to TLS data.





313

314 **Figure 3.** Log-log regression equations and  $r^2$  values for prediction of specific leaf area (SLA) derived

315 leaf area index (LAI) by terrestrial laser scanning (TLS) derived metrics: A) shrub height, B) canopy

316 cover, C) height \* canopy cover, D) TLS leaf area, E) voxel volume, and F) convex hull volume.

317

318 However, the convex hull and point-intercept sampling methods provided comparable

319 results and this demonstrates the fine-scale capabilities of the TLS and the capacity to replace

320 time-consuming field techniques. TLS also has the potential to scale from field to airborne or

321 satellite-based measurements. The TLS provides point data similar to point-intercept sampling,  
322 yet uses the same technology and delivers a similar 3-D point cloud to airborne laser scanning  
323 (ALS). TLS could be used as ground validation for ALS, in which simple metrics such as  
324 vegetation height (Luo et al., 2015) or percent vegetation cover can be calculated from lower  
325 density ALS data, and could be used for future work estimating sagebrush LAI across the  
326 landscape. For example, Mitchell et al. (2011) found height and canopy cover for sagebrush were  
327 consistently underestimated when using moderate resolution ALS data (9.46 pts m<sup>-2</sup>) but with  
328 compensation, accurate estimates of both shrub height ( $r^2 = 0.86$ ) and canopy cover ( $r^2 = 0.78$ )  
329 could be obtained. A hierarchical method linking ground estimates to TLS, and TLS to ALS,  
330 may provide the ability to scale up from the plot to the watershed level (Li et al., 2015). Further,  
331 as ALS technology improves to higher point densities, volume measurements will become more  
332 accurate (Vierling et al., 2013) and more viable for estimating plant characteristics such as LAI  
333 and biomass.

334 Monitoring of vegetation structure and function at the plot-level (i.e., hectare) and  
335 landscape-level (i.e., tens to hundreds of km<sup>2</sup>) may also be accomplished with a combination of  
336 spectral and structural remote-sensing data. Estimation of vegetation characteristics in dryland  
337 ecosystems with spectral information alone (e.g., Landsat multispectral or AVIRIS hyperspectral  
338 data) has proven difficult due to high levels of land cover heterogeneity and pixel mixing (Okin  
339 et al., 2001). Yet, hyperspectral imagery with up to a hundred or more spectral bands has been  
340 shown to be useful, especially when combined with structural information from ALS (Mitchell et  
341 al., 2015). For species-specific parameters, hyperspectral imagery can provide species-level  
342 classification and top of canopy spectral information, while TLS or ALS provides the structural  
343 information necessary to capture multiple levels of canopy structure. Correspondingly, TLS-

344 derived LAI could readily promote estimates of photosynthesis and evapotranspiration, which  
345 are crucial variables for climate change research. For example, within and between seasonal  
346 changes in LAI might be obtained by TLS due to its portability and relative ease-of-use in the  
347 field. These changes of LAI over time could then be used to estimate how evapotranspiration of  
348 sagebrush communities change in the context of warming (Polley et al., 2013). Furthermore LAI,  
349 coupled with measurements of vegetation function, such as nitrogen from hyperspectral data will  
350 help model CO<sub>2</sub> uptake in these systems (Mitchell et al., 2012). Expanded ground-based LAI  
351 measurements in dryland shrub environments will improve our ability to develop and estimate  
352 LAI products at the airborne and satellite scales. Spatially-explicit models of LAI, derived from  
353 laser data acquired at these broader scales, can help with reducing uncertainties associated with  
354 carbon and water flux models in drylands and detecting subtle ecosystem responses to  
355 disturbance over time.

### 356 *3.3. Conclusions*

357 Findings from this study support those at other sites and with other shrub species, which  
358 indicate SLA can be site specific. Consequently, SLA sampling is advisable for new sites,  
359 particularly those in differing climatic and edaphic conditions, rather than simply accepting and  
360 applying published average values. More importantly, we demonstrated that models involving  
361 TLS-derived canopy volume, canopy cover, or laser-reflectance values (i.e., green vs. non-green  
362 points) can explain 65-76% of the variance in SLA-derived LAI of sagebrush. A 3-D convex hull  
363 analysis provided the most accurate prediction ( $r^2 = 0.76$ ) of SLA-derived LAI using TLS data.  
364 This performance was quite similar to that obtained using a traditional field technique, point-  
365 intercept sampling but at what is likely a substantial reduction in field-time costs.

366           These results, coupled with previous studies (e.g., Greaves et al., 2015; Olsoy et al.,  
367 2014) suggest that TLS is a promising technology for quantifying vegetation structure in shrub-  
368 dominated landscapes. With further validation of larger shrubs (e.g. > 1 m<sup>2</sup>) and additional  
369 woody species, TLS may be a rapid and accurate tool for indirectly measuring LAI in dryland  
370 shrub environments.

371

### 372 **Acknowledgements**

373           This study was funded by NSF EAR 1355702 and NOAA OAR Earth Systems Research  
374 Laboratory/ Physical Sciences Division NA10OAR4680240. We thank Mr. Randy Lee at Idaho  
375 National Laboratory for his assistance with the TLS.

376 **References**

- 377 Ackerly, D.D., Knight, C.A., Weiss, S.B., Barton, K., Starmer, K.P., 2002. Leaf size, specific  
378 leaf area and microhabitat distribution of chaparral woody plants: contrasting patterns in  
379 species level and community level analyses. *Oecologia* 130, 449–457.
- 380 Backlund, P., Schimel, D., Janetos, A., Hatfield, J., Ryan, M.G., Archer, S.R., Lettenmaier, D.,  
381 2008. The effects of climate change on agriculture, land resources, water resources, and  
382 biodiversity in the United States. Washington, DC, USA.
- 383 Barber, C.B., Dobkin, D.P., Huhdanpaa, H., 1996. The quickhull algorithm for convex hulls.  
384 *ACM Trans. Math. Softw.* 22, 469–483. doi:10.1145/235815.235821
- 385 Bates, J.D., Svejcar, T., Miller, R.F., Angell, R.A., 2006. The effects of precipitation timing on  
386 sagebrush steppe vegetation. *J. Arid Environ.* 64, 670–697.  
387 doi:10.1016/j.jaridenv.2005.06.026
- 388 Beerling, D.J., Fry, J.C., 1990. A comparison of the accuracy, variability and speed of five  
389 different methods for estimating leaf area. *Ann. Bot.* 65, 483–488.
- 390 Beland, M., Baldocchi, D.D., Widlowski, J.-L., Fournier, R.A., Verstraete, M.M., 2014. On  
391 seeing the wood from the leaves and the role of voxel size in determining leaf area  
392 distribution of forests with terrestrial LiDAR. *Agric. For. Meteorol.* 184, 82–97.
- 393 Bonan, G.B., 1993. Importance of leaf area index and forest type when estimating photosynthesis  
394 in boreal forests. *Remote Sens. Environ.* 43, 303–314. doi:10.1016/0034-4257(93)90072-6
- 395 Bonham, C.D., 1989. *Measurements for terrestrial vegetation*. John Wiley and Sons, New York,  
396 NY.
- 397 Branson, F.A., Miller, R.F., McQueen, I.S., 1976. Moisture relationships in twelve northern  
398 desert shrub communities near Grand Junction, Colorado. *Ecology* 57, 1104–1124.
- 399 Breda, N.J., 2003. Ground-based measurements of leaf area index: a review of methods,  
400 instruments and current controversies. *J. Exp. Bot.* 54, 2403–2417.
- 401 Breshears, D.D., 2006. The grassland-forest continuum, trends in ecosystem properties for  
402 woody plant mosaics. *Front. Ecol. Environ.* 4, 96–104.
- 403 Bussotti, F., Pollastrini, M., 2015. Evaluation of leaf features in forest trees: methods,  
404 techniques, obtainable information and limits. *Ecol. Indic.* 52:219–230.
- 405 Cheng, T., Rivard, B., Sánchez-Azofeifa, A. G., Féret, J. B., Jacquemoud, S., Ustin, S. L. 2014.  
406 Deriving leaf mass per area (LMA) from foliar reflectance across a variety of plant species  
407 using continuous wavelet analysis. *ISPRS J. Photogramm. Remote Sens.* 87, 28–38.

- 408 Chiarriello, N.R., Mooney, H.A., Williams, K., 1989. Growth, carbon allocation and cost of plant  
409 tissues, in: Pearcy, R.W., Ehleringer, J., Mooney, H.A., Rundel, P. (Eds.), *Plant*  
410 *Physiological Ecology: Field Methods and Instrumentation*. Chapman and Hall, London, pp.  
411 327–365.
- 412 Cifuentes, R., Van der Zande, D., Farifteh, J., Salas, C., Coppin, P., 2014. Effects of voxel size  
413 and sampling setup on the estimation of forest canopy gap fraction from terrestrial laser  
414 scanning data. *Agric. For. Meteorol.* 194, 230–240.
- 415 Clark, P.E., Seyfried, M.S., 2001. Point sampling for leaf area index in sagebrush steppe  
416 communities. *J. Range Manag.* 54, 589–594.
- 417 Cleary, M.B., Pendall, E., Ewers, B.E., 2008. Testing sagebrush allometric relationships across  
418 three fire chronosequences in Wyoming, USA. *J. Arid Environ.* 72, 285–301.  
419 doi:10.1016/j.jaridenv.2007.07.013
- 420 Danson, F.M., Rowland, C.S., Baret, F., 2003. Training a neural network with a canopy  
421 reflectance model to estimate crop leaf area index. *Int. J. Remote Sens.* 24, 4891–4905.
- 422 Enquist, B.J., Brown, J.H., West, G.B., 1998. Allometric scaling of plant energetics and  
423 population density. *Nature* 395, 163–165.
- 424 Finzel, J.A., Seyfried, M.S., Wertz, M.A., Kiniry, J.R., Johnson, M.V., Launchbaugh, K.L., 2012.  
425 Indirect measurement of leaf area index in sagebrush-steppe rangelands. *Rangel. Ecol.*  
426 *Manag.* 65, 208–212. doi:10.2111/REM-D-11-00069.1
- 427 Flerchinger, G.N., Hanson, C.L., Wight, J.R., 1996. Modeling evapotranspiration and surface  
428 energy budgets across a watershed. *Water Resour. Res.* 32, 2539–2548.  
429 doi:10.1029/96WR01240
- 430 García, M., Gajardo, J., Riaño, D., Zhao, K., Martín, P., Ustin, S., 2015. Canopy clumping  
431 appraisal using terrestrial and airborne laser scanning. *Remote Sens. Environ.* 161, 78–88.
- 432 Gower, S.T., Kucharik, C.J., Norman, J.M., 1999. Direct and indirect estimation of leaf area  
433 index, fAPAR, and net primary production of terrestrial ecosystems. *Remote Sens. Environ.*  
434 70, 29–51.
- 435 Greaves, H.E., Vierling, L.A., Eitel, J.U.H., Boelman, N.T., Magney, T.S., Prager, C.M., Griffin,  
436 K.L., 2015. Estimating aboveground biomass and leaf area of low-stature Arctic shrubs with  
437 terrestrial LiDAR. *Remote Sens. Environ.* 164, 26–35.
- 438 Hoffman, T.L., Wambolt, C.L., 1996. Growth response of Wyoming big sagebrush to heavy  
439 browsing by wild ungulates, in: Barrow, J.R., McArthur, E.D., Sosebee, R.E., Tausch, R.J.  
440 (Eds.), *Proceedings: Shrubland Ecosystem Dynamics in a Changing Environment*. USDA,  
441 Forest Service, Intermountain Research Station, Las Cruces, NM, pp. 242–245.

- 442 Hopkinson, C., Lovell, J., Chasmer, L., Jupp, D., Kljun, N., van Gorsel, E., 2013. Integrating  
443 terrestrial and airborne lidar to calibrate a 3D canopy model of effective leaf area index.  
444 *Remote Sens. Environ.* 136, 301–314. doi:10.1016/j.rse.2013.05.012
- 445 Hosoi, F., Omasa, K., 2006. Voxel-based 3-D modeling of individual trees for estimating leaf  
446 area density using high-resolution portable scanning lidar. *IEEE Trans. Geo. Remote Sens.*  
447 44, 3610–3618.
- 448 Hosoi, F., Omasa, K., 2007. Factors contributing to accuracy in the estimation of the woody  
449 canopy leaf area density profile using 3D portable lidar imaging. *J. Exp. Bot.* 58, 3463–  
450 3473. doi:10.1093/jxb/erm203
- 451 Hufkens, K., Bogaert, J., Dong, Q.H., Lu, L., Huang, C.L., Ma, M.G., Che, T., Li, X.,  
452 Veroustraete, F., Ceulemans, R. 2008. Impacts and uncertainties of upscaling remote-  
453 sensing data validation for a semi-arid woodland. *J. Arid Environ.* 72, 1490–1505.  
454 doi:10.1016/j.jaridenv.2008.02.012
- 455 Hunt Jr., E.R., Everitt, J.H., Ritchie, J.C., Moran, M.S., Booth, D.T., Anderson, G.L., Clark,  
456 P.E., Seyfried, M.S., 2003. Applications and research using remote sensing for rangeland  
457 management. *Photogramm. Eng. Remote Sens.* 69, 675–693. doi:10.14358/PERS.69.6.675
- 458 Jonckheere, I., Fleck, S., Nackaerts, K., Muys, B., Coppin, P., Weiss, M., Baret, F., 2004.  
459 Review of methods for in situ leaf area index determination: Part I. Theories, sensors and  
460 hemispherical photography. *Agric. For. Meteorol.* 121, 19–35.
- 461 Kremer, R.G., Running, S.W., 1993. Community type differentiation using NOAA / AVHRR  
462 data within a sagebrush-steppe ecosystem. *Remote Sens. Environ.* 46, 311–318.
- 463 Kwon, H., Pendall, E., Ewers, B.E., Cleary, M., Naithani, K., 2008. Spring drought regulates  
464 summer net ecosystem CO<sub>2</sub> exchange in a sagebrush-steppe ecosystem. *Agric. For.*  
465 *Meteorol.* 148, 381–391. doi:10.1016/j.agrformet.2007.09.010
- 466 Levia, D.F., 2008. A generalized allometric equation to predict foliar dry weight on the basis of  
467 trunk diameter for eastern white pine (*Pinus strobus* L.). *For. Ecol. Manage.* 255, 1789–  
468 1792.
- 469 Li, A., Glenn, N.F., Olsoy, P.J., Mitchell, J.J., Shrestha, R., 2015. Aboveground biomass  
470 estimates of sagebrush using terrestrial and airborne LiDAR data in a dryland ecosystem.  
471 *Agric. For. Meteorol.* 213, 138–147. doi:10.1016/j.agrformet.2015.06.005
- 472 Luo, S., Wang, C., Pan, F., Xi, X., Li, G., Nie, S., Xia, S., 2015. Estimation of wetland  
473 vegetation height and leaf area index using airborne laser scanning data. *Ecol. Indic.* 48,  
474 550–559.
- 475 Meigs, P., 1953. World distribution of arid and semi-arid homoclimates. *Rev. Res. Arid Zo.*  
476 *Hydrol. UNESCO doc*, 203–209.

- 477 Mitchell, J.J., Glenn, N.F., Sankey, T.T., Derryberry, D.R., Anderson, M.O., Hruska, R.C., 2011.  
478 Small-footprint Lidar estimations of sagebrush canopy characteristics. *Photogramm. Eng.*  
479 *Remote Sens.* 77, 521–530.
- 480 Mitchell, J.J., Glenn, N.F., Sankey, T.T., Derryberry, D.R., Germino, M.J., 2012. Remote  
481 sensing of sagebrush canopy nitrogen. *Remote Sens. Environ.* 124, 217–223.  
482 doi:10.1016/J.Rse.2012.05.002
- 483 Mitchell, J.J., Shrestha, R., Spaete, L.P., Glenn, N.F., 2015. Combining airborne lidar and  
484 hyperspectral data across local sites for upscaling shrubland structural information: lessons  
485 for HypSPIRI. *Remote Sens. Environ.* 167, 98–110. doi:10.1016/j.rse.2015.04.015
- 486 Mundt, J.T., Streutker, D.R., Glenn, N.F., 2006. Mapping sagebrush distribution using fusion of  
487 hyperspectral and lidar classifications. *Photogramm. Eng. Remote Sens.* 72, 47–54.  
488 doi:10.14358/PERS.72.1.47
- 489 Mussche, S., Samson, R., Nachtergale, L., De Schrijver, A., Lemeur, R., Lust, N., 2001. A  
490 comparison of optical and direct methods for monitoring the seasonal dynamics of leaf area  
491 index in deciduous forests. *Silva Fenn.* 35, article id 575.
- 492 Okin, G.S., Roberts, D.A., Murray, B., Okin, W.J., 2001. Practical limits on hyperspectral  
493 vegetation discrimination in arid and semiarid environments. *Remote Sens. Environ.* 77,  
494 212–225. doi:10.1016/S0034-4257(01)00207-3
- 495 Olsoy, P.J., Glenn, N.F., Clark, P.E., Derryberry, D.R., 2014. Aboveground total and green  
496 biomass of dryland shrub derived from terrestrial laser scanning. *ISPRS J. Photogramm.*  
497 *Remote Sens.* 88, 166–173. doi:10.1016/j.isprsjprs.2013.12.006
- 498 Ordoñez, J.C., van Bodegom, P.M., Witte, J.-P.M., Wright, I.J., Reich, P.B., Aerts, R., 2009. A  
499 global study of relationships between leaf traits climate and soil measures of nutrient  
500 fertility. *Global Ecol. Biogeogr.* 18, 137–149.
- 501 Pfennigbauer, M., 2010. Improving quality of laser scanning data acquisition through calibrated  
502 amplitude and pulse deviation measurement. *Proc. SPIE*, 7684, 76841F.
- 503 Polley, H.W., Briske, D.D., Morgan, J.A., Wolter, K., Bailey, D.W., Brown, J.R., 2013. Climate  
504 change and North American rangelands: Trends, projections, and implications. *Rangel.*  
505 *Ecol. Manag.* 66, 493–511. doi:10.2111/REM-D-12-00068.1
- 506 Poorter, H., Remkes, C., 1990. Leaf area ratio and net assimilation rate of 24 wild species  
507 differing in relative growth rate. *Oecologia* 83, 553–559.
- 508 Prater, M.R., DeLucia, E.H., 2006. Non-native grasses alter evapotranspiration and energy  
509 balance in Great Basin sagebrush communities. *Agric. For. Meteorol.* 139, 154–163.  
510 doi:10.1016/j.agrformet.2006.08.014



- 511 Pugnaire, F.I., Haase, P., Puigdefabregas, J., 1996. Facilitation between higher plant species in a  
512 semiarid environment. *Ecology* 77, 1420–1426.
- 513 Qi, J., Chehbouni, A., Huete, A.R., Kerr, Y.H., 1994. Modified soil adjusted vegetation index  
514 (MSAVI). *Remote Sens. Environ.* 48, 119–126.
- 515 Qi, J., Kerr, Y.H., Moran, M.S., Weltz, M., Huete, A.R., Sorooshian, S., Bryant, R., 2000. Leaf  
516 area index estimates using remotely sensed data and BRDF models in a semiarid region.  
517 *Remote Sens. Environ.* 73, 18–30.
- 518 Qi, Y., Dennison, P. E., Jolly, W. M., Kropp, R. C., Brewer, S. C. 2014. Spectroscopic analysis  
519 of seasonal changes in live fuel moisture content and leaf dry mass. *Remote Sens.*  
520 *Environ.* 150, 198–206.
- 521 R Core Team, 2013. R: A language and environment for statistical computing [WWW  
522 Document]. R Found. Stat. Comput. Vienna, Austria. URL <http://www.r-project.org/>
- 523 Reekie, E.G., Reekie, J.Y.C., 1991. The effect of reproduction on canopy structure, allocation  
524 and growth in *Oenothera biennis*. *Ecology* 79, 1061–1071.
- 525 Riegl, 2015. Riegl VZ-1000 data sheet 2015-03-24 [PDF Document]. Riegl Laser Measurement  
526 Systems GmbH, Horn, Austria. URL  
527 [http://www.riegl.com/uploads/tx\\_pxpriegldownloads/DataSheet\\_VZ-1000\\_2015-03-24.pdf](http://www.riegl.com/uploads/tx_pxpriegldownloads/DataSheet_VZ-1000_2015-03-24.pdf)  
528 (accessed 6.26.15).
- 529 Serbin, S. P., Singh, A., McNeil, B. E., Kingdon, C. C., Townsend, P. A. 2014. Spectroscopic  
530 determination of leaf morphological and biochemical traits for northern temperate and  
531 boreal tree species. *Ecol. Appl.* 24, 1651–1669.
- 532 Smith, M.O., Ustin, S.L., Adams, J.B., Gillespie, A.R., 1990. Vegetation in deserts: I. A regional  
533 measure of abundance from multispectral images. *Remote Sens. Environ.* 31, 1–26.
- 534 Soil Survey Staff, 2013. Web Soil Survey [WWW Document]. Nat. Resour. Conserv. Serv.  
535 United State Dep. Agric. URL <http://websoilsurvey.nrcs.usda.gov/> (accessed 4.17.13).
- 536 Turner, D.P., Cohen, W.B., Kennedy, R.E., Fassnacht, K.S., Briggs, J.M., 1999. Relationship  
537 between leaf area index and Landsat TM spectral vegetation indices across three temperate  
538 zone sites. *Remote Sens. Environ.* 70, 52–68.
- 539 Vierling, L.A., Xu, Y., Eitel, J.U.H., Oldow, J.S., 2013. Shrub characterization using terrestrial  
540 laser scanning and implications for airborne LiDAR assessment. *Can. J. Remote Sens.* 38,  
541 709–722. doi:10.5589/m12-057
- 542 Whittaker, R.H., Woodwell, G.M., 1967. Surface area relations of woody plants and forest  
543 communities. *Am. J. Bot.* 54, 931–939.

- 544 Wight, J.R., Hanson, C.L., Cooley, K.R., 1986. Modeling evapotranspiration from sagebrush-  
545 grass rangeland. *J. Range Manag.* 39, 81–85.
- 546 WRCC, 2009. Idaho climate summaries [WWW Document]. West. Reg. Clim. Center, Desert  
547 Res. Inst. URL <http://www.wrcc.dri.edu/summary/climsmid.html>
- 548 Yang, J., Weisberg, P.J., Bristow, N.A., 2012. Landsat remote sensing approaches for monitoring  
549 long-term tree cover dynamics in semi-arid woodlands: comparison of vegetation indices  
550 and spectral mixture analysis. *Remote Sens. Environ.* 119, 62–71.
- 551 Yang, R., Xianghong, H., Liu, J., Wu, H., 2012. Research on the three angular resolution of  
552 terrestrial laser scanning. *International Archives of the Photogrammetry, Remote Sensing  
553 and Spatial Information Sciences*, Volume XXXIX-B3, XXII ISPRS Congress, 25 August –  
554 01 September 2012, Melbourne, Australia.

